Anthropogenic Impacts on Global Storage and Emissions of Mercury from Terrestrial Soils: Insights from a New Global Model

JOURNAL OF GEOPHYSICAL RESEARCH, VOL. 115, G03008, doi:10.1029/2009JG001124, 2010

Anthropogenic impacts on global storage and emissions of mercury from terrestrial soils: Insights from a new global model

Nicole V Smith-Downey,[1,2] Elsie M. Sunderland,[1,3] and Daniel J. Jacob[1,3]

Received 16 August 2009; revised 5 March 2010; accepted 22 March 2010; published 20 July 2010.

[1] We develop a mechanistic global model of soil mercury storage and emissions that ties the lifetime of mercury in soils to the lifetime of the organic carbon pools it is associated with. We explore the implications of considering terrestrial mercury cycling in the framework of soil carbon cycling and suggest possible avenues of future research to test our assumptions and constrain this type of model. In our simulation, input of mercury to soil is by atmospheric deposition, in part through leaf uptake and subsequent litter fall, and is moderated by surface photoreduction and revolatilization. Once bound to organic carbon, mercury is transferred along a succession of short-lived to long-lived carbon pools and is ultimately reemitted by respiration of these pools. We examine the legacy of anthropogenic influence on global mercury storage and emissions and estimate that storage of mercury in organic soils has increased by ~20% since preindustrial times, while soil emissions have increased by a factor of 3 (2900 Mg yr^{-1} versus 1000 Mg yr^{-1}). At steady state, mercury accumulates in the most recalcitrant soil carbon pools and has an overall lifetime against respiration of 630 years. However, the impact of anthropogenic emissions since preindustrial times has been concentrated in more labile pools, so that the mean lifetime of present-day anthropogenic mercury in all pools is ~80 years. Our analysis suggests that reductions in anthropogenic emissions would lead to immediate and large reductions in secondary soil mercury emissions.

Citation: Smith-Downey, N. V, E. M. Sunderland, and D. J. Jacob (2010), Anthropogenic impacts on global storage and emissions of mercury from terrestrial soils: Insights from a new global model, *J. Geophys. Res.*, *115*, G03008, doi:10.1029/2009JG001124.

1. Introduction

[2] Exposure of humans and wildlife to methylmercury at high levels causes a variety of negative health effects [*Mergler et al.*, 2007]. Several studies attribute substantial increases in mercury levels in wildlife since industrialization to nonlocal anthropogenic mercury emissions [*Fitzgerald and Clarkson*, 1991; *Fitzgerald et al.*, 1991; *Lindqvist et al.*, 1991; *Monteiro and Furness*, 2005; *Dietz et al.*, 2006]. *Mason and Sheu* [2002] estimate that global emissions of natural and previously deposited anthropogenic mercury from terrestrial ecosystems account for >1600 Mg yr^{-1} and are comparable in magnitude to annual anthropogenic emissions (2200 Mg yr^{-1}). Sediment archives suggest that anthropogenic mercury sources have increased deposition to terrestrial systems by at least a factor of 3 [*Lorey and Driscoll*, 1999; *Swain et al.*, 1992], while global models suggest that the surface soil reservoir may have increased by 10%–15% since industrialization [*Mason et al.*, 1994; *Mason and Sheu*, 2002; *Selin et al.*, 2008]. Although the atmosphere has been most enriched by anthropogenic mercury emissions, the largest reservoirs of mercury are contained in terrestrial soils, sediments, and subsurface ocean waters [*Mason and Sheu*, 2002; *Selin et al.*, 2008; *Sunderland and Mason*, 2007]. The goal of this paper is to explore the implications of considering terrestrial mercury cycling in the framework of soil carbon cycling, to estimate the possible magnitude of anthropogenic mercury emissions on soil storage and fluxes, and to suggest avenues for future research to test the parameters that control mercury storage in this framework. We do this by developing a global scale mechanistic representation of mercury cycling in soils and exchange with the atmosphere linking mercury dynamics to the dynamics of soil organic carbon pools.

[3] Anthropogenic emissions of mercury are primarily in the form of elemental mercury (Hg^0), divalent mercury (Hg(II)), and particulate mercury (Hg(p)). Hg^0 is relatively volatile and insoluble in water, whereas Hg(II) is less volatile and extremely soluble. This imparts mercury with an atmospheric cycle largely controlled by its redox chemistry. Hg^0 in the atmosphere can be oxidized to Hg(II), which is then rapidly deposited to the land or ocean surface. Hg(II) can then be reduced to Hg^0 and reemitted to the atmosphere. Estimates of the lifetime of Hg^0 in the atmosphere range from 0.7 to

[1]Faculty of Arts and Sciences, Harvard University, Cambridge, Massachusetts, USA.
[2]Now at Jackson School of Geosciences, University of Texas, Austin, Texas, USA.
[3]School of Engineering and Applied Sciences, Harvard University, Cambridge, Massachusetts, USA.

0148-0227/10/2009JG001124

1.7 years [*Mason et al.*, 1994; *Bergan et al.*, 1999; *Shia et al.*, 1999; *Lamborg et al.*, 2002; *Mason and Sheu*, 2002; *Seigneur et al.*, 2004; *Selin et al.*, 2007], leading to transport on a global scale. This cycle of deposition and reemission pumps mercury through the land-ocean-atmosphere system until it reaches a long-lived reservoir.

[4] In this study, we distinguish between four types of mercury emissions from soils. Primary natural emissions are derived directly from the lithosphere on long time scales by weathering of the mineral fraction of soils and intermittently by large emissions from volcanic eruptions. Secondary natural emissions are derived from primary natural mercury that has been deposited to the land surface and reemitted. Primary anthropogenic emissions are derived from the lithosphere and are emitted during industrial processes such as coal combustion, metal smelting, and waste incineration. Secondary anthropogenic emissions are derived from primary anthropogenic mercury that has been deposited to the land surface and reemitted. Secondary emissions are not well quantified and yet are critical for understanding the natural mercury cycle and the legacy of anthropogenic emissions.

[5] We divide soil mercury into three classes depending on its association in the soil matrix: mineral mercury (contained in the soil mineral fraction), mercury loosely adsorbed to the surface of soil particles, and mercury bound to organic carbon complexes (O-Hg). Mineral mercury is derived directly from soil parent material (rock), and although the mercury content is relatively low (~10 ng g^{-1} [*Friedli et al.*, 2007]), the high density and large volume of mineral soils globally make this the largest pool of mercury in the environment. The distribution of mineral mercury is highly spatially variable and is related to rock type [*Schroeder et al.*, 2005]. The release of mercury from the mineral pool to the atmosphere is controlled by weathering on long time scales and, intermittently, by large emissions from volcanic activity.

[6] The second pool, loosely adsorbed/surface mercury, is derived from atmospheric deposition of Hg(II) and Hg^0 to soil and leaf surfaces. Hg(II) can bind to negatively charged soil particles, but this bond is relatively weak and processes such as cation and water addition can displace Hg(II) from soils and lead to evasion [*Farella et al.*, 2006]. This pool is relatively short lived and is one source of secondary soil emissions. Hg^0 is not stored in background soils on long time scales and is revolatilized to the atmosphere.

[7] The third soil pool, organically bound mercury (O-Hg), is derived from atmospheric deposition to soils and leaves. It originates from the incorporation mercury into leaf tissue, followed by litterfall and wet deposition and throughfall of Hg(II). Hg(II) binds to reduced sulfur groups in soil organic matter with very high affinity [*Skyllberg et al.*, 2000; *Haitzer et al.*, 2003; *Khwaja et al.*, 2006] and is protected against reduction until the organic matter is respired [*Wickland et al.*, 2006; *Fritsche et al.*, 2008] or consumed by fire [*Friedli et al.*, 2003; *Turetsky et al.*, 2006; *Wiedinmyer and Friedli*, 2007]. We argue that organically bound mercury is of central importance for understanding soil-atmosphere mercury dynamics, because it is the pool that stores terrestrial mercury deposition on a time scale of months to years. The controls on the lifetime and turnover of this pool therefore control the mass of mercury in surface soils that interacts with the atmosphere.

[8] Since the vast majority of atmospherically derived mercury in soils is associated with organic carbon, we argue that organic carbon cycling processes that operate on time scales of months to decades control the lifetime and fate of atmospherically derived soil mercury [*Grigal*, 2003; *Wickland et al.*, 2006; *Obrist*, 2007]. The deposition of mercury to the land surface and subsequent incorporation into the O-Hg pool are not a permanent mercury sink, rather, mercury will be released as soil organic matter proceeds through the stages of decomposition or when soils are burned. The concentration of mercury in soils is therefore a function of the deposition rate and carbon turnover time.

[9] Here we quantify the storage and reemission of atmospherically derived mercury in soils by developing a new global model of mercury cycling in terrestrial systems. Our soil mercury model is based on the CASA biogeochemical model, a well-established framework for simulating ecosystem carbon dynamics [*Potter et al.*, 1993; *van der Werf et al.*, 2003, 2006]. The main objective of this research is to better characterize impacts of anthropogenic mercury and climate processes on soil mercury storage and emissions. To do this, we supply our model with mercury deposition fluxes from the GEOS-Chem global chemical transport model [*Selin et al.*, 2007, 2008]. We constrain the model using observed soil mercury measurements and evaluate the impact of anthropogenic mercury emissions on the storage and emissions of mercury from soils. We then evaluate the differences in lifetime between newly deposited mercury and background mercury in soils.

2. Global Terrestrial Mercury Model (GTMM)

[10] The global terrestrial mercury model (GTMM) is a global 1° × 1° biogeochemical model of mercury accumulation and emissions that we apply to the continuous evolution of soil mercury from preindustrial to present day with a monthly time step. Figure 1 presents an overview of the model. Mercury is deposited to the land surface as either wet deposition of Hg(II) or dry deposition of Hg(II) and Hg^0. Monthly deposition of Hg(II) and Hg^0 are taken from the mercury simulation in the GEOS-Chem chemical transport model [*Selin et al.*, 2008]. GEOS-Chem also includes a small deposition flux of Hg(p) emitted by combustion; this Hg(p) is not considered available for terrestrial cycling. In the model, dry deposition of Hg^0 and Hg(II) can be fixed into the interior of leaves or remain on leaf and soil surfaces. Hg(II) on leaf and soil surfaces is subject to photoreduction, and Hg^0 is subject to revolatilization. Wet deposition of Hg(II) and Hg(II) washed off of leaf and soil surfaces enters soils and can bind to reduced sulfur groups in organic material. At this point, the cycling of mercury in organic soils is controlled by the cycling of carbon and is modeled within the carbon cycling framework of the CASA biogeochemical model [*Potter et al.*, 1993; *van der Werf et al.*, 2003, 2006].

[11] We use the GEOS-Chem mercury simulation as described by *Selin et al.* [2008] to supply monthly, spatially resolved, and speciated dry and wet mercury deposition fluxes to the GTMM. The simulation includes 3-D atmospheric transport coupled to 2-D surface ocean and land reservoirs. The atmospheric component uses assimilated meteorological data from the NASA Goddard Earth Observing System (GEOS-4) to drive transport and chemistry at 4° × 5° horizontal resolution [*Bey et al.*, 2001]. The surface ocean reservoir cycles with the atmosphere on a 1 year time

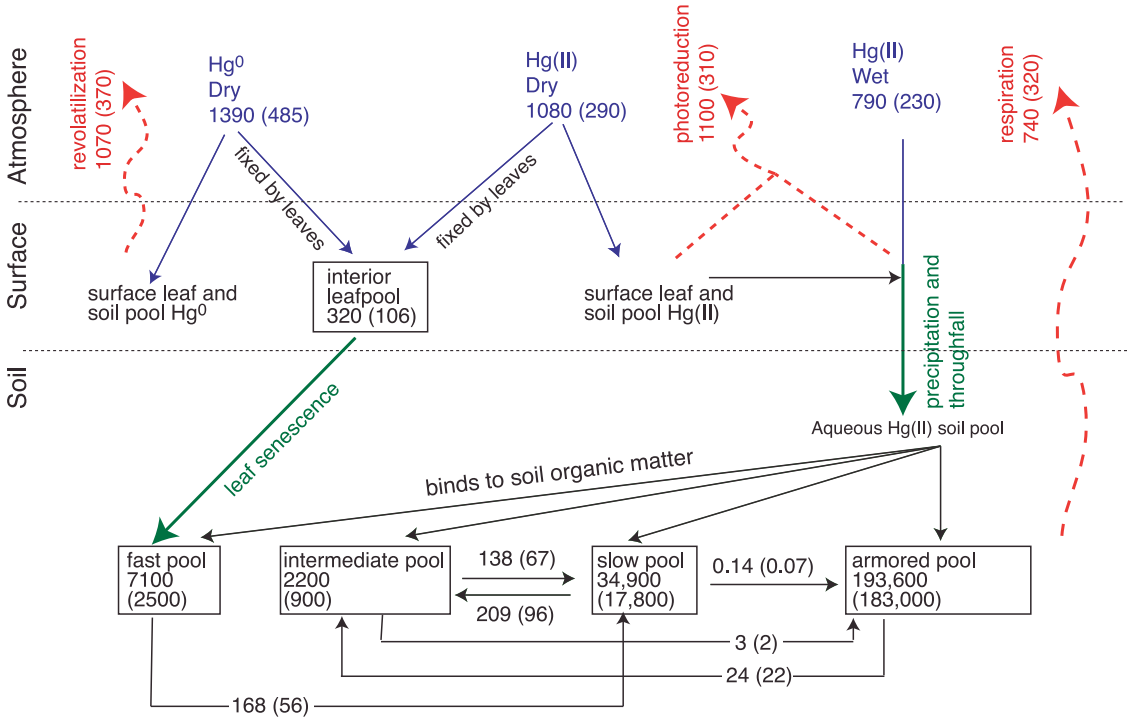

Figure 1. Schematic of the global terrestrial mercury model (GTMM). Boxes represent pools tied to carbon cycling in the model. Numbers in the boxes give the present-day storage of mercury (Mg), and other numbers give mercury fluxes in and out of pools (Mg yr^{-1}). Numbers in parenthesis are preindustrial values. Deposition of Hg^0 and Hg(II) are taken from the GEOS-Chem mercury simulation [*Selin et al.*, 2008]. Mercury enters organic soils by either leaf senescence or washoff and wet deposition of Hg(II) (green arrows). Soils emit mercury to the atmosphere via revolatilization, photoreduction, and respiration (red arrows).

scale and with a deep ocean of prescribed concentrations [*Strode et al.*, 2007]. The land reservoir in the original *Selin et al.* [2008] model cycles with the atmosphere by prompt reemission of mercury deposited to vegetation but does not actually store mercury in soil. The model contains a constant primary natural source of 500 Mg Hg yr^{-1} attributed to rock weathering and volcanoes [*Lindqvist et al.*, 1991], which is highly uncertain, particularly given that volcanic emissions are extremely large and infrequent. The GEOS-Chem Hg^0 and Hg(II) dry deposition fluxes are from a canopy resistance-in-series model [*Wang et al.*, 1998; *Wesely*, 1989] that includes uptake by leaf stomata and cuticles as a function of land cover type, leaf area index (LAI), stomatal resistance (function of temperature and light), water solubility (measured by the Henry's law constant), and chemical reactivity (measured by a "reactivity factor"). The reactivity factor of 10^{-5} is assumed to match observed deposition velocities for Hg^0 [*Selin et al.*, 2007, 2008, and references therein]. Specified Henry's law constants in GEOS-Chem are 1×10^6 M atm^{-1} for Hg(II) and 0.11 M atm^{-1} for Hg^0 [*Lin et al.*, 2006]. The GEOS-Chem atmospheric chemistry simulation generally compares well to data [*Selin et al.*, 2007], particularly for wet deposition over the United States [*Selin and Jacob*, 2008].

[12] *Selin et al.* [2008] previously applied GEOS-Chem to reconstruct the global biogeochemical cycle of mercury for preindustrial (steady state) and present-day (taken as 2000) conditions. The total modeled mercury deposition to land (excluding perennially ice covered surfaces) is 1000 Mg yr^{-1} for preindustrial and 3300 Mg yr^{-1} for present day (Figure 2).

[13] For input to GTMM, we need the temporal evolution of these deposition fluxes over the industrial period in order to track the time-dependent evolution of anthropogenic mercury in soil reservoirs. To our knowledge, the only available historical inventory of primary anthropogenic emissions over the industrial period is for North America [*Pirrone et al.*, 1998]. We assume that the *Pirrone et al.* [1998] relative trend of anthropogenic emissions applies globally and further assume that the present-day speciation of emissions in GEOS-Chem [from *Pacyna et al.*, 2006] applies to the historical record (Figure 3). This is clearly an oversimplification, but it serves our purpose of exploring the time-dependent legacy of anthropogenic mercury in soils in a general sense.

[14] We conduct GEOS-Chem simulations to calculate mercury deposition fluxes for six historical points along that record: 1840, 1905, 1925, 1941, 1970, and 2000. 1840 and 2000 are taken as the preindustrial and present-day conditions. For each point, we conduct 3 year GEOS-Chem simulations with 2000–2002 meteorology (to smooth out interannual variability), preceded by a 3 year initialization to allow fast equilibration of the atmosphere, surface ocean, and vegetation [*Selin et al.*, 2008]. Secondary anthropogenic emission from soils in GEOS-Chem is assumed to follow the trend of cumulative anthropogenic emissions in Figure 3, applied as scaling factors to the 2000 simulation. We use the same meteorology for all historical points so that differences

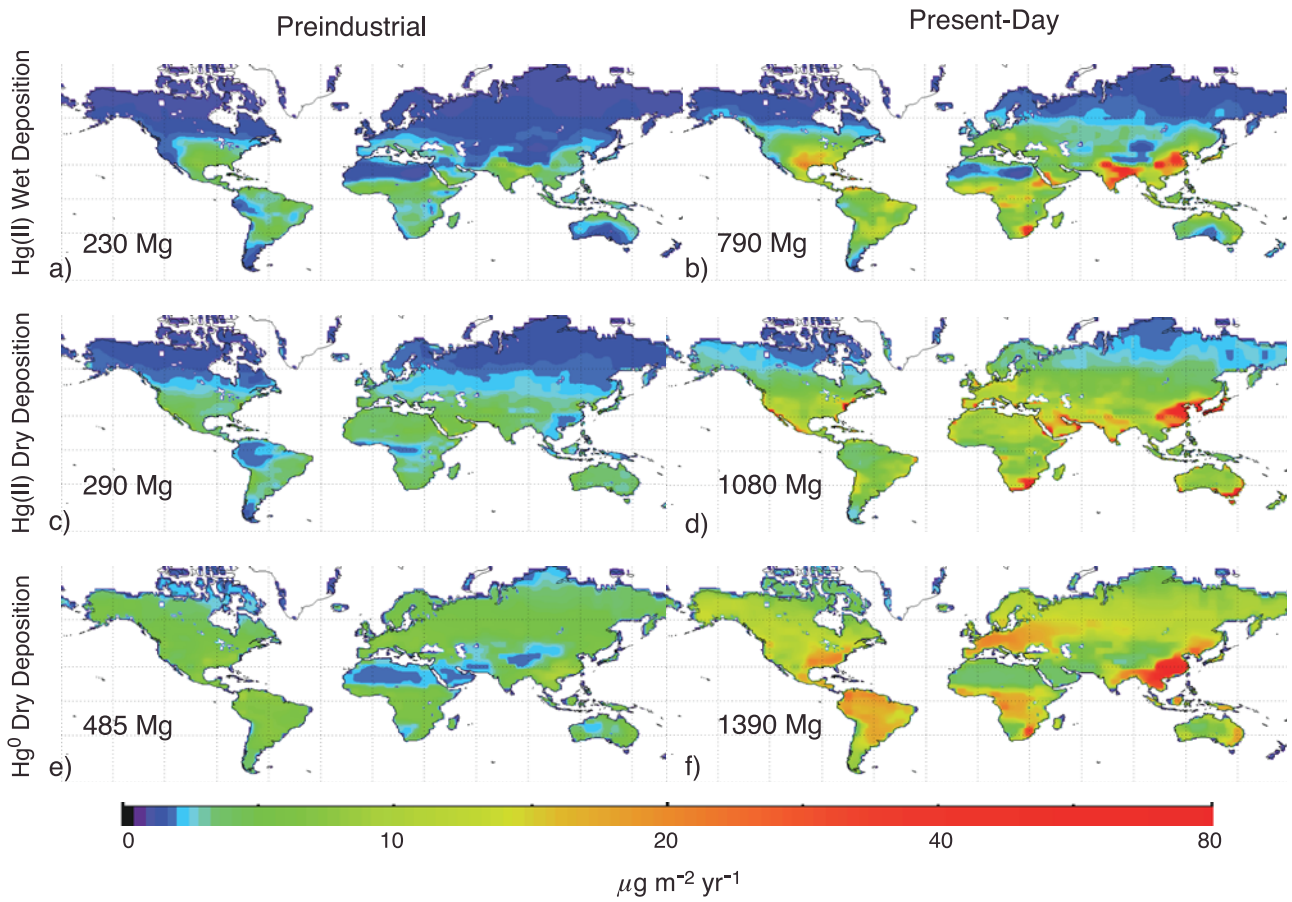

Figure 2. Mercury deposition fluxes to land (excluding perennially ice covered surfaces) from the GEOS-Chem simulation for preindustrial and present day. Numbers in the panels are annual totals.

between points are solely driven by anthropogenic emissions. We fit splines to the archived speciated fluxes from GEOS-Chem to generate a continuous record of speciated monthly deposition to land from 1840 to 2000 and regrid the fluxes 1° × 1° resolution for input to GTMM. The total cumulative global anthropogenic mercury emissions we estimate from 1840 to 2000 are 219,000 Mg.

[15] The CASA biogeochemical model uses a combination of assimilated meteorological data and remote sensing observations to predict the spatial and temporal distribution of net carbon fluxes in terrestrial ecosystems [*Potter et al.*, 1993]. The net accumulation of carbon by plants globally or net primary production (NPP) is estimated as a function of solar radiation flux (s), the fraction of light absorbed by the plant canopy (FPAR), and the light use efficiency (ε), which is a function of temperature (T) and soil moisture (M) [*Field et al.*, 1995, 1998]:

$$\mathrm{NPP} = \varepsilon(T, M) \cdot s \cdot \mathrm{FPAR}. \quad (1)$$

For this analysis, we used the version of the CASA model developed by *van der Werf et al.* [2003, 2006] to calculate carbon fluxes and added mercury to the simulation. We used mean monthly estimates of s and T from the GEOS-4 assimilated meteorological data averaged for 2000–2002 on the 1° × 1° CASA grid. Soil moisture (M) is calculated

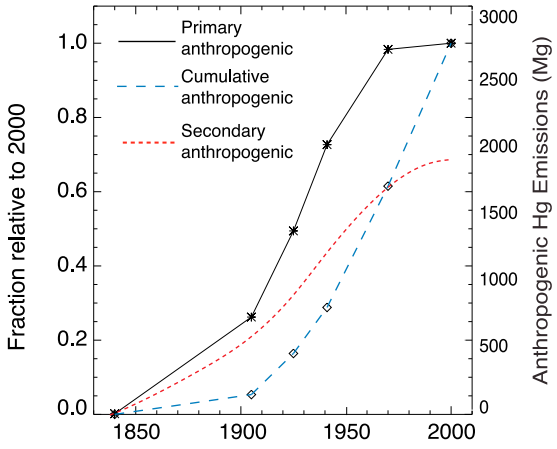

Figure 3. Assumed historical trend of global anthropogenic emissions based on the *Pirrone et al.* [1998] historical inventory for North America and annual emissions of primary and secondary anthropogenic mercury for the period 1840–2000. Values are shown as scaling factors relative to 2000 for direct primary anthropogenic emissions and for cumulative emissions (integral of primary emissions). Symbols identify the six emission years for which GEOS-Chem deposition fields are calculated.

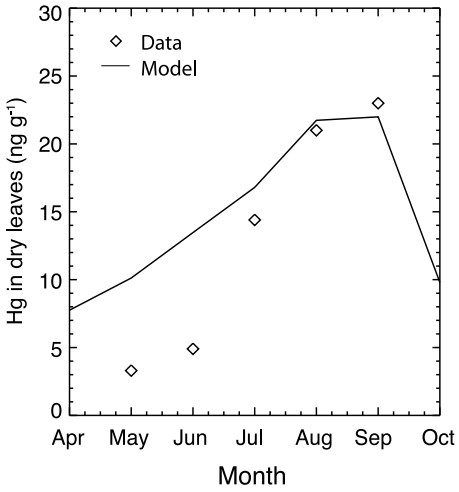

Figure 4. Seasonal mercury accumulation in leaves at the Lake Huron Watershed site in Michigan (45.57°N, 84.80°W). Observations from *Rea et al.* [2002] are compared to model results.

within CASA as a function of soil texture, precipitation, and evapotranspiration [*Potter et al.*, 1993]. *FPAR* is a function of leaf cover and is estimated from satellite remote sensing of the normalized difference vegetation index (NDVI) from SeaWiFs for 1997–2000, as described by *Behrenfeld et al.* [2001].

[16] CASA calculates decomposition of litter and soil organic matter storage for the top 30 cm of soils as a function of temperature, soil moisture, soil texture, and C/N ratio (or litter quality). Temperature and precipitation are from the GEOS-4 assimilated meteorological data. Satellite-derived estimates of NDVI are used to drive the seasonality of leaf out, leaf senescence, and delivery of fine roots to litter pools [*Randerson et al.*, 1996].

[17] The soil carbon dynamics in CASA are based on the CENTURY model [*Parton et al.*, 1987], which tracks carbon pools based on their characteristic turnover time rather than their physical location in the soil profile [*Potter et al.*, 1993]. There are four major classes of soil carbon pools including fast turnover, intermediate turnover, slow turnover, and armored pools (Figure 1). In each time step, CASA estimates the transfer of carbon between pools and the fluxes of carbon to the atmosphere from decomposition. The version of CASA we are using [*van der Werf et al.*, 2003, 2006] also simulates carbon emissions from biomass burning, but the soil burning schemes have not been optimized, so for this study, we have not directly estimated mercury fluxes from soil combustion.

3. Mercury Soil Accumulation and Reemission Processes

[18] Field measurements show that leaves accumulate mercury over the growing season [*Rea et al.*, 2002; *Stamenkovic and Gustin*, 2009] and laboratory enrichment experiments show that nearly all of the mercury in leaves is derived from the atmosphere and not from soils [*Ericksen et al.*, 2003; *Gustin et al.*, 2004]. Deposited mercury can be permanently fixed into leaf tissue [*Ericksen et al.*, 2003; *Ericksen and Gustin*, 2004; *Millhollen et al.*, 2006; *Graydon et al.*, 2009], and this mercury remains in leaves until the end of the growing season when they are shed to the soil surface.

[19] We assume that some fraction of mercury from dry deposition is permanently fixed by leaves (f_{fixed}), and we use measurements of mercury accumulation in leaves over a growing season at Lake Huron Watershed in Michigan [*Rea et al.*, 2002] to parameterize f_{fixed} as a function of leaf area index (LAI) assuming no wet deposition contribution to leaf mercury:

$$f_{\text{fixed}} = \begin{cases} 0.25 \cdot \dfrac{\text{LAI}}{1.25}, \text{LAI} \leq 1.25 \\ 0.25, \text{LAI} > 1.25 \end{cases}. \quad (2)$$

In this case, total mercury fixed by leaves is equal to the product of f_{fixed} and the total Hg^0 and Hg(II) dry deposition. Figure 4 compares the resulting modeled and observed Hg/C content of leaves at the site over the course of the growing season. The model overestimates the initial buildup but reproduces the observed accumulation at the end of the growing season, which determines the litter flux. Although this may be an oversimplification of the leaf-scale processes that drive mercury accumulation over the growing season, parameterizing leaf uptake as a function of LAI gives us the flexibility to model this process with respect to a parameter that is easily measured in the field.

[20] Unbound elemental mercury does not significantly contribute to the total mercury found in background soils [*Skyllberg et al.*, 2000; *Friedli et al.*, 2007], so in our model all dry deposition of Hg^0 that is not permanently incorporated into leaf tissue is revolatilized to the atmosphere (hereafter referred to as revolatilization). Both dry and wet deposition of Hg(II) to leaf and soil surfaces are subject to photoreduction (if not permanently fixed by leaves), and we parameterize this flux (hereafter referred to as photoreduction) as a function of light intensity based on data reported by *Rolfhus and Fitzgerald* [2004],

$$f_{\text{photoreduction}} = 0.67 \cdot (1 - e^{-0.016 \cdot s}), \quad (3)$$

where $f_{\text{photoreduction}}$ is the fraction of Hg(II) deposited to leaf and soil surfaces that is reemitted to the atmosphere and s is the solar radiation flux (W m^{-2}). The remaining dry deposition of Hg(II) (minus leaf uptake and photoreduction) resides in the surface leaf/soil pool and is washed off in precipitation events (Figure 1). This is equivalent to the throughfall flux measured in field experiments.

[21] We assume that Hg(II) delivered to soils by wet deposition and washoff from vegetation and soil surfaces binds to organic material with a limit set by the local carbon pool size. We calculate that there are 1.2×10^{-4} M reduced sulfur groups available for Hg(II) binding per gram carbon in soils [*Qian et al.*, 2002] and that wet deposited Hg(II) binds to each soil organic matter pool with equal affinity [*Skyllberg et al.*, 2003]. This amounts to a maximum storage of 2.4×10^{-2} g Hg/g C. We find that the supply of binding sites for mercury is generally not a limiting factor for mercury incorporation in the soil.

[22] The Hg/C ratio in soils reflects a balance between mercury binding to soil carbon and release when this carbon decomposes. We assume that during decomposition, mercury associated with carbon can either be reduced to Hg^0 or remain

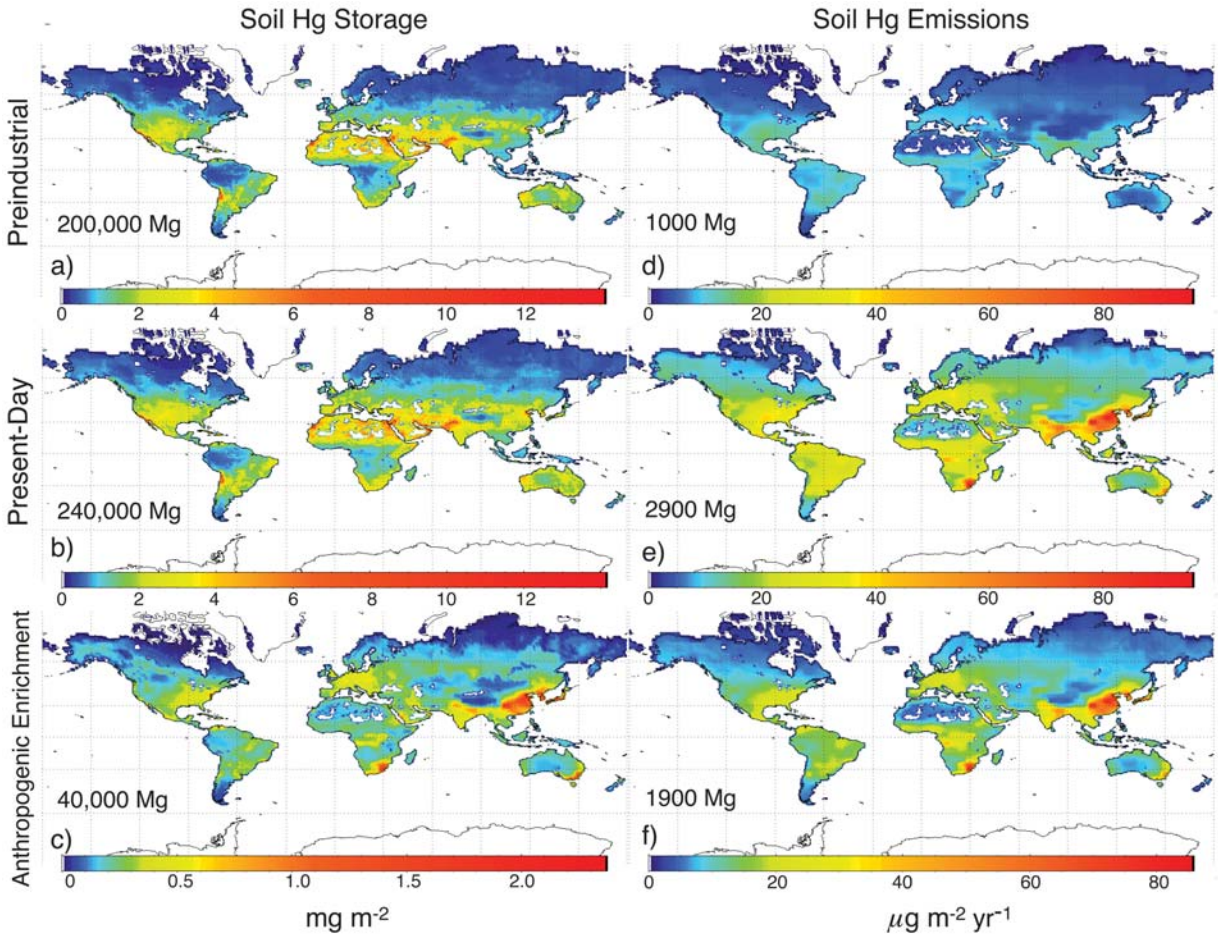

Figure 5. Soil storage and emissions of mercury in soils simulated by the model for preindustrial and present-day conditions. The anthropogenic enrichment computed as the difference between the two.

attached to the pool. The fraction of mercury released as Hg^0 is f_{decomp}. We used Hg/C soil measurements along transects in the United States [*Smith et al.*, 2005] to constrain f_{decomp} in the model. To estimate soil Hg/C content, we ran the soil model to equilibrium with preindustrial speciated mercury deposition fields. Once the soil model reached equilibrium (~30,000 years), we ramped up emissions as described above using monthly deposition estimates from 1840 to 2000. The *Smith et al.* [2005] soil transects found a mean ratio of 3×10^{-7} g Hg/g C in the organic horizon of soils, and we find that $f_{decomp} = 0.16$ provides the best match to the observed soil Hg/C ratios.

4. Results and Discussion

[23] From the above-described preindustrial equilibrium simulation, we find that the preindustrial steady state content of organically bound mercury in soils was 200,000 Mg globally. This is lower than total soil mercury estimates, which are ~1,000,000 Mg mercury [*Mason and Sheu*, 2002; *Sunderland and Mason*, 2007], reflecting the dominance of the mineral component of soil in the mercury budget. The global distribution of soil mercury storage and emissions for both preindustrial and present-day simulations is shown in Figure 5. The relatively low soil mercury concentrations in boreal and arctic ecosystems are driven by extremely low deposition (Table 1). The high soil concentrations in desert ecosystems are driven by a combination of higher deposition and extremely slow mercury turnover (Table 1). Preindustrial soil emissions balance deposition of mercury to the soil surface by assumption of steady state. The total soil emission of 1000 Mg yr^{-1} is composed of 370 Mg yr^{-1} from revolatilization, 320 Mg yr^{-1} from respiration, and 310 Mg yr^{-1} from photoreduction (Figure 1). We assume that the carbon cycle has remained in steady state over the industrial period.

[24] At steady state, mercury is concentrated in the most recalcitrant (armored) pool (90%), followed by the slow pool (9%), the fast pool (1%), and the intermediate pool (0.5%) (Figure 6). Our assumption that mercury binds to all soil pools with equal affinity, combined with f_{decomp} much less than 1, leads to the accumulation of mercury in the most recalcitrant pools. Field and laboratory experiments in the aquatic environment show little preference between carbon classes in mercury binding efficiency [*Skyllberg et al.*, 2003], and reduced sulfur binding sites available for Hg(II) are far in excess of background mercury concentrations [*Qian et al.*, 2002], so we have some confidence in our assumption. *Obrist et al.* [2009] report that the ratio of Hg/C in organic

Table 1. Summary of Biome Level Hg Deposition and Soil Hg Turnover Times

	Mean Hg Deposition (g/m^2)		Mean Soil Hg Turnover Time[a] (years)	
	Preindustrial	Present day	Preindustrial	Present day
Tropical Forest	0.9	2.7	234	126
Temperate Forest	0.8	2.9	250	151
Boreal Forest	0.5	1.5	998	560
Grassland	1.0	3.5	522	269
Tundra	0.3	0.8	1108	702
Desert	0.5	1.4	2387	1748

[a]With respect to respiration.

soils increases through the stages of decomposition in four Sierra Nevada forest sites, which they suggest could be due to either a low fraction of mercury emitted during decomposition or continued addition of mercury to soil pools through their stages of decomposition, both of which are consistent with our model. Although we have assumed that f_{decomp} = 0.16 for all cases, future field and laboratory experiments will likely show that it varies with carbon pool, biome, and/or environmental conditions.

[25] Although mercury is concentrated in the most recalcitrant soil pools, respiration emissions at steady state are driven by the more labile pools (Figure 6). In our simulation, we find that anthropogenic emissions of mercury have increased organically bound mercury in soils to 240,000 Mg (20%) by the year 2000 (Figure 5). Organic soils have therefore stored ~ 20% of anthropogenic mercury emissions since 1840. In the present-day scenario, soil emissions nearly triple to 2900 Mg yr^{-1}. *Mason and Sheu* [2002] previously estimated that soil mercury storage increased by 86,000 Mg and emissions increased by 800 Mg from preindustrial to the present day. They found that terrestrial emissions have approximately doubled, whereas we find that they have tripled.

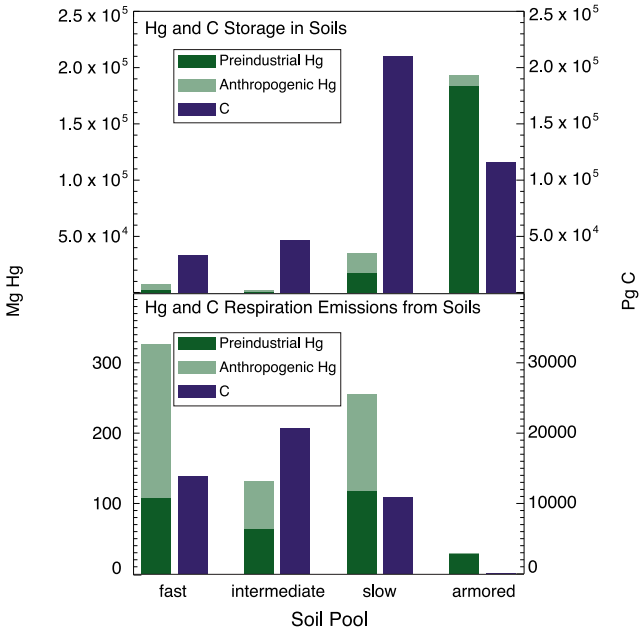

Figure 6. Storage and emissions of mercury and carbon for individual soil pools in the CASA model. Dark green bars for mercury are preindustrial values, and light green bars are the present-day anthropogenic additions. Blue bars are carbon.

[26] Our model suggests that the largest mass changes since preindustrial times have occurred in the slow cycling carbon pool (Figure 6) and the largest relative increase in mercury content occurred in the fast pool (Figure 7), which saw a factor of 2.9 increase in mercury content from 1840 to 2000. This was followed by the intermediate pool (2.1), slow pool (1.7), and armored pool (1.1). This implies that the local impact of anthropogenic mercury loading on soil emissions and storage will depend heavily on the carbon-cycling rate and is driven by our assumption that mercury binds to all soil pools with equal affinity. If, however, future field or laboratory experiments show that mercury binds preferentially to younger (or older) soil pools, these conclusions will need to be reevaluated. By the year 2000, secondary emissions of anthropogenic mercury are 1900 Mg yr^{-1} (Figure 3). The ratio of secondary to primary anthropogenic emissions decreases over time (Figure 3), reflecting the transfer of anthropogenic mercury to longer-lived carbon pools.

[27] Emissions of mercury by photoreduction and revolatilization respond instantaneously to changes in deposition and, hence, to primary anthropogenic emissions, which level off after 1970 (Figure 8). The respiration flux responds much

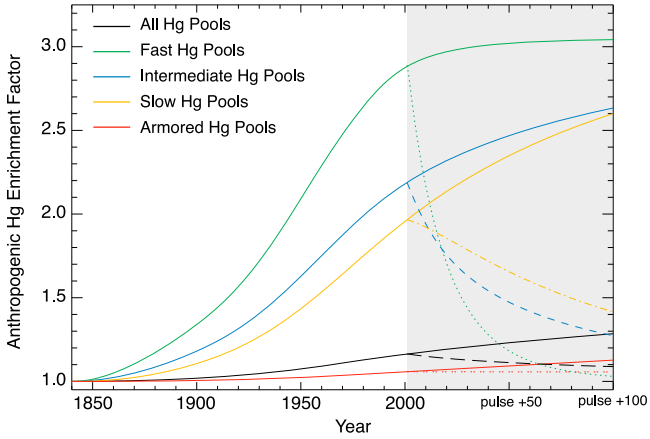

Figure 7. Relative anthropogenic enrichment factor for each soil pool from the preindustrial to present day (2000). Gray shading represents the trajectory of the anthropogenic enrichment factor in soils given a continuation of deposition at 2000 levels (solid lines). Dotted lines show the decay of the anthropogenic enrichment factor for mercury stored in soils at the present day. This suggests that emissions reductions would lead to immediate and large decreases in the anthropogenic enrichment factor in the most labile pools. Increases in emissions (not shown) would lead to an increase in the anthropogenic enrichment factor for all pools.

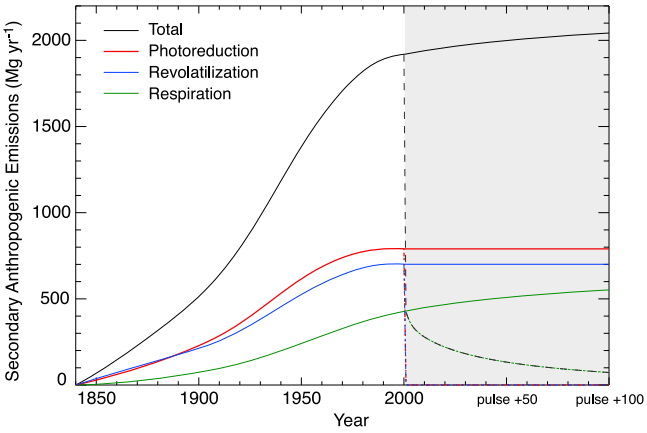

Figure 8. Secondary anthropogenic emissions of mercury by mechanism for preindustrial through present day (2000). Gray shading represents the trajectory of emissions given constant deposition (solid lines) and shows the decay of emissions for mercury stored in soils at the present day (dotted lines).

more slowly and continues to increase at a relatively constant rate after 1970. In the present-day scenario, total mercury deposition to the land surface is 3254 Mg yr^{-1} and total soil mercury emissions are 2900 Mg yr^{-1}.

[28] We find that the anthropogenic mercury perturbation to the steady state preindustrial simulation decreases the total lifetime of mercury in soils from a mean of 631 to 323 years (Figure 9) and that anthropogenic mercury in the present day has a mean lifetime of 80 years. We see that the lifetime of mercury with respect to respiration is longest in tundra and desert ecosystems, where respiration is very low, and shortest in tropical and temperate ecosystems (Table 1). Tropical and temperate lifetimes are similar despite the faster carbon turnover in tropical systems due to the relative balance between mercury supplied by wet deposition versus leaf uptake. In our simulation, mercury supplied by wet deposition (which dominates in tropical systems) has a longer relative lifetime because we assume that it binds to all carbon pools, whereas mercury incorporated into leaf tissue has a shorter lifetime because it is transferred directly to the fast pool and follows the same trajectory as carbon entering via leaves.

[29] The legacy of anthropogenic mercury presently stored in soils, and the potential response to emissions reductions can be examined in an idealized simulation shutting off anthropogenic mercury deposition (return to preindustrial deposition) immediately after the present day. Over time, as anthropogenic mercury is removed preferentially from the most labile pools (shaded region, Figure 7), we see a decrease in soil storage (Figure 10a) and a rapid decrease in soil mercury emissions (Figure 10b). Because soil emissions are primarily driven by mercury contained in the most labile pools (Figure 6), as anthropogenic mercury is transferred to the more long-lived pools emissions decrease rapidly, and are composed of only respiration emissions after the first year (shaded region, Figure 8). This translates into a lengthening of the lifetime of anthropogenic mercury in soils over time (Figure 10c). This simplistic experiment suggests that anthro-

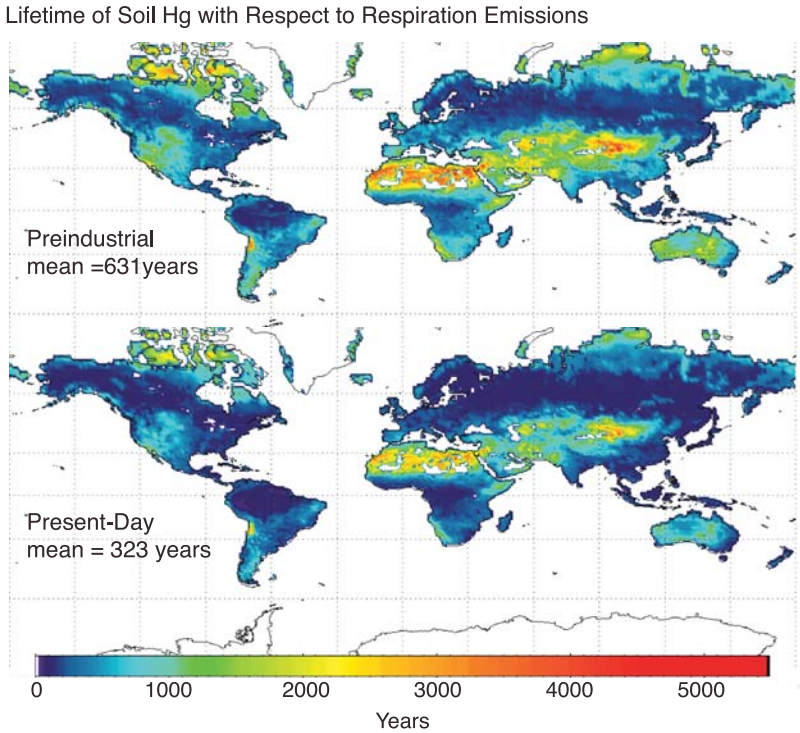

Figure 9. Lifetime of soil mercury with respect to respiration emissions for the preindustrial and present-day scenarios. The mean lifetime of the anthropogenic mercury enrichment in all pools for the present-day scenario is 80 years.

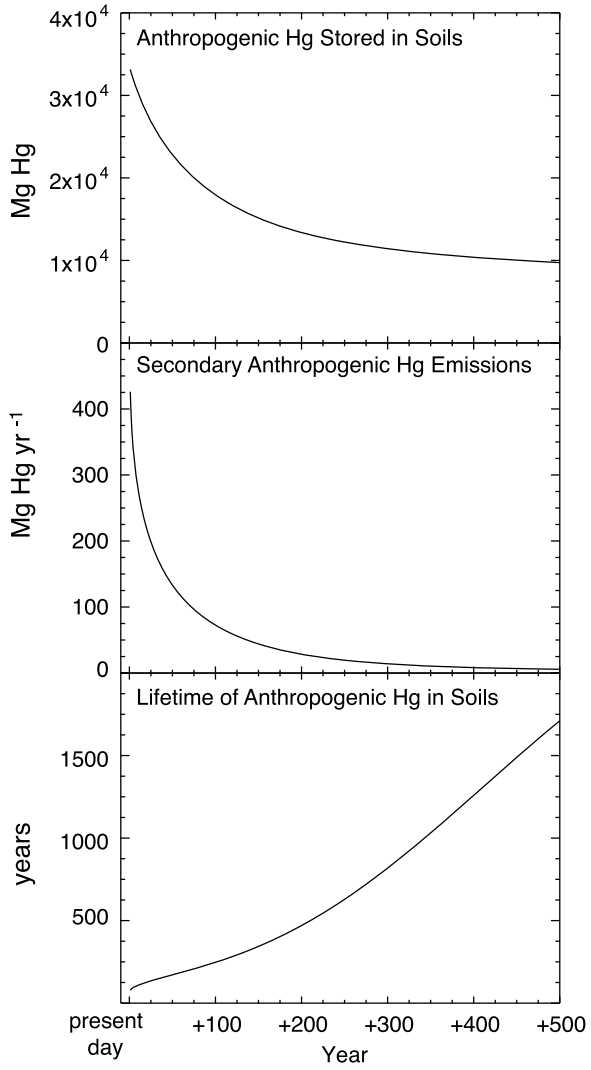

Figure 10. Decay of soil storage and emissions of anthropogenic mercury in a simulation assuming no anthropogenic deposition (return to preindustrial deposition) after the year 2000. The evolution of the lifetime of anthropogenic mercury in soil is also shown.

pogenic emissions reductions would lead to immediate and large reductions in mercury concentrations in the most labile pools and reductions in emissions from soils.

[30] The limitations of this type of large-scale modeling approach are numerous. Operating at a 1° × 1° grid scale allows us to evaluate the model globally across all biomes, but the subgrid scale variability that is important for both mercury and carbon cycling cannot be captured. The CASA model has been broadly applied to estimate global carbon fluxes and generally performs well [*Malmstrom et al.*, 1997; *Cramer et al.*, 1999; *Ruimy et al.*, 1999]. Small-scale soil characteristics such as redox potential are not resolved by CASA, and there is no mechanism for tracking the physical depth of carbon/mercury stored in soil, which is an important parameter, particularly for fires [*Carrasco et al.*, 2006; *Turetsky et al.*, 2006]. Additionally, the even larger grid scale (4° × 5°) for mercury deposition estimates precludes us from realistically simulating ecosystem level mercury fluxes at a finer resolution. This type of model is useful, however, to evaluate the conceptual implications of considering soil mercury cycling in the context of soil carbon cycling, to evaluate the terrestrial mercury cycle in that framework, and to suggest possible avenues of future research that will help to more tightly constrain the parameters we have used. This framework can be applied to mercury modeling at multiple scales in the future (i.e., from site level to watershed to global) and should be a useful analogue for mercury cycling in aquatic systems.

[31] Our simulation is particularly sensitive to the parameters f_{fixed}, $f_{\text{photoreduction}}$, and f_{decomp} and our assumption that Hg(II) binds with equal affinity to soil carbon pools of all ages. None of these parameters are well constrained with existing data, but this model was specifically constructed with parameters that could be measured in the field. We hope that in the future, more field and laboratory experiments can refine these parameterizations (or suggest new ones) and improve the simulation. We did not include error bar estimates in this analysis due to the lack of strong constraints on our parameters. Of primary importance is to determine whether mercury in soils binds to all soil pools with equal affinity, which we assume here. If, for example, mercury binds with a higher affinity to more labile pools, the distribution of mercury in soils will more closely resemble that of carbon and the lifetime will be shorter.

[32] Because we have not taken fire into account in this model, the lifetime of mercury in soils for fireprone areas is an upper estimate. *Friedli et al.* [2009] estimated that annual mercury emissions from fires are 675 ± 240 Mg over the period 1997–2006, with the largest emissions occurring in tropical and boreal Asia. They highlight the possibility that increasing temperatures in boreal regions may significantly increase emissions of mercury from biomass burning, which would also lead to a decrease in the lifetime. Any disturbance, such as fire or land use change, that reduces the carbon lifetime in soils will correspondingly reduce the lifetime (and storage) of mercury in soils. Despite the limitations listed here, this model is an important conceptual step forward in understanding the terrestrial mercury cycle.

5. Conclusions

[33] The goal of this paper was to explore the implications of considering soil mercury cycling in the framework of soil carbon cycling, and here we present a model that accounts for the mechanistic cycling and fluxes of mercury within terrestrial ecosystems and exchange with the atmosphere. Here we used the connection between mercury and soil organic carbon to combine a model of ecosystem carbon fluxes (CASA) with a global model of speciated mercury deposition (GEOS-Chem). This approach allowed us to describe the lifetime and turnover of mercury in soils based on the lifetime and turnover of the soil carbon pool to which it is bound. Developing a process-based model that tracks mercury dynamics in terrestrial systems improves our ability to describe present-day mercury cycling and allows us to make predictions about the response of terrestrial mercury cycling to future climate and land use change. Our model suggests that organically bound mercury in preindustrial soils was 200,000 Mg, and that there has been a 20% increase in organically bound soil mercury (to 240,000 Mg) from preindustrial steady state conditions to the present day.

[34] Fractionally, the most labile organically bound mercury pools have been more heavily impacted by anthropogenic mercury emissions than more recalcitrant pools. This implies that the present-day lifetime of anthropogenic mercury in soils is shorter than that of natural mercury (80 years versus 631 years) because it is a transient perturbation that has not yet reached steady state. Emissions from the most labile pool account for ~40% of the total soil mercury emissions to the atmosphere in the present-day scenario and are nearly triple their preindustrial value. Because this pool is in rapid equilibration with the atmosphere, decreases in deposition will lead to rapid decreases in the storage and emissions of mercury from the most labile pools, leading to an increase in the lifetime of anthropogenic mercury as it is transferred to more recalcitrant pools. Although the bulk soil mercury pool will be slow to respond in terms of mass (Figure 7), reductions in anthropogenic mercury emissions will target the most labile pools and will lead to rapid reductions in soil mercury emissions. Because the most labile pools are preferentially decomposed and methylated (*Moreau et al.*, in preparation), reductions in anthropogenic mercury emissions should have an immediate effect on both soil emission rates and ecosystem level methylation rates.

[35] The rate of carbon cycling in an ecosystem will be an important driver of the long-term evolution of anthropogenically derived mercury pollution. Additionally, changing the carbon cycling rate of an area through land use, disturbance, or climate change will alter the lifetime of mercury in soils. Any process that results in rapid carbon loss (such as fire, or transition from saturated to unsaturated conditions) will lead to rapid mercury loss as well. The potential for climate change to significantly increase soil mercury emissions via increased respiration or soil burning is clear. The modeling framework presented here is a useful tool for evaluating the temporal and spatial evolution of mercury storage and emissions. The association between soil organic carbon and soil mercury storage provides a powerful framework to evaluate terrestrial mercury cycling.

[36] **Acknowledgments.** N.S.-D. gratefully acknowledges support as a Beagle Environmental Fellow through the Harvard University Center for the Environment and thanks G. v.d.Werf and J. Randerson for assistance with CASA. D.J.J acknowledges support from the Atmospheric Chemistry Program of the National Science Foundation and the U. S. Environmental Protection Agency.

References

Behrenfeld, M., et al. (2001), Biospheric primary production during an ENSO transition, *Science*, *291*, 2594–2597.

Bergan, T., L. Gallardo, and H. Rodhe (1999), Mercury in the global troposphere: A three-dimensional model study, *Atmos. Environ.*, *33*, 1575–1585.

Bey, I., D. J. Jacob, R. M. Yantosca, J. A. Logan, B. D. Field, A. M. Fiore, Q. Li, H. Y. Liu, L. J. Mickley, and M. G. Schultz (2001), Global modeling of tropospheric chemistry with assimilated meteorology: Model description and evaluation, *J. Geophys. Res.*, *106*, 23,073–23,095, doi:10.1029/2001JD000807.

Carrasco, J. J., J. C. Neff, and J. W. Harden (2006), Modeling physical and biogeochemical controls over carbon accumulation in a boreal forest soil, *J. Geophys. Res.*, *111*, G02004, doi:10.1029/2005JG000087.

Cramer, W., D. W. Kicklighter, A. Bondeau, B. Moore, G. Churkina, B. Nemry, A. Ruimy, and A. L. Schloss (1999), Comparing global models of terrestrial net primary productivity (NPP): overview and key results, *Global Change Biol.*, *5*, 1–15.

Dietz, R., et al. (2006), Trends in mercury in hair of Greenlandic polar bears (*Ursus maritimus*) during 1892–2001, *Environ. Sci. Technol.*, *40*, 1120–1125, doi:10.1021/es051636z.

Ericksen, J. A., and M. S. Gustin (2004), Foliar exchange of mercury as a function of soil and air mercury concentrations, *Sci. Total Environ.*, *324*, 271–279, doi:10.1016/jscitotenv.200310.034.

Ericksen, J. A., M. S. Gustin, D. E. Schorran, D. W. Johnson, S. E. Lindberg, and J. S. Coleman (2003), Accumulation of atmospheric mercury in forest foliage, *Atmos. Environ.*, *37*(12), 1613–1622.

Farella, N., M. Lucotte, R. Davidson, and S. Daigle (2006), Mercury release from deforested soils triggered by base cation enrichment, *Sci. Total Environ.*, *368*, 19–29.

Field, C. B., J. T. Randerson, and C. M. Malmstrom (1995), Ecosystem net primary production: combining ecology and remote sensing, *Remote Sens. Environ.*, *51*, 75–88.

Field, C. B., M. J. Behrenfeld, J. T. Randerson, and P. Falkowski (1998), Primary productivity of the biosphere: an integration of terrestrial and oceanic components, *Science*, *281*, 237–240.

Fitzgerald, W. F., and T. W. Clarkson (1991), Mercury and monomethylmercury: Present and future concerns, *Environ. Health Persp.*, *96*, 159–166.

Fitzgerald, W. F., R. P. Mason, and G. M. Vandal (1991), Atmospheric cycling and air-water exchange of mercury over mid-continental lacustrine regions, *Water Air Soil Poll.*, *56*, 745–767.

Friedli, H. R., L. F. Radke, J. Y. Lu, C. M. Banic, W. R. Leaitch, and J. I. MacPherson (2003), Mercury emissions from burning of biomass from temperate North American forests: laboratory and airborne measurements, *Atmos. Environ.*, *37*(2), 253–267.

Friedli, H. R., L. F. Radke, N. J. Payne, D. J. McRae, T. J. Lynham, and T. W. Blake (2007), Mercury in vegetation and organic soil at an upland boreal forest site in Prince Albert National Park, Saskatchewan, Canada, *J. Geophys. Res.*, *112*, G01004, doi:10.1029/2005JG000061.

Friedli, H. R., A. F. Arellano, S. Cinnirella, and N. Pirrone (2009), Initial estimates of mercury emissions to the atmosphere from global biomass burning, *Environ. Sci. Technol.*, *43*, 3507–3513.

Fritsche, J., D. Obrist, and C. Alewell (2008), Evidence of microbial control of Hg-0 emissions from uncontaminated terrestrial soils, *J. Plant Nutr. Soil Sci.*, *171*, 200–209, doi:10.1002/jpln.200625211.

Graydon, J. A., V. L. St. Louis, H. Hintelmann, S. E. Lindberg, K. A. Sandilands, J. Rudd, C. A. Kelly, M. T. Tate, D. P. Krabbenhoft, and I. Lehnherr (2009), Investigation of uptake and retention of atmospheric Hg(II) by boreal forest plants using stable Hg isotopes, *Environ. Sci. Technol.*, *43*, 4960–4966.

Grigal, D. F. (2003), Mercury sequestration in forests and peatlands: A review, *J. Environ. Qual.*, *32*(2), 393–405.

Gustin, M. S., J. A. Ericksen, D. E. Schorran, D. W. Johnson, S. E. Lindberg, and J. S. Coleman (2004), Application of controlled mesocosms for understanding mercury air-soil-plant exchange, *Environ. Sci. Technol.*, *38*, 6044–6050.

Haitzer, M., G. R. Aiken, and J. N. Ryan (2003), Binding of mercury(II) to aquatic humic substances: Influence of pH and source of humic substances, *Environ. Sci. Technol.*, *37*(11), 2436–2441.

Khwaja, A. R., P. R. Bloom, and P. L. Brezonik (2006), Binding constants of divalent mercury (Hg^{2+}) in soil humic acids and soil organic matter, *Environ. Sci. Technol.*, *40*, 844–849.

Lamborg, C. H., W. F. Fitzgerald, J. O'Donnell, and T. Torgersen (2002), A non-steady-state compartmental model of global-scale mercury biogeochemistry with interhemispheric gradients, *Geochim. Cosmochim. Acta.*, *66*(7), 1105–1118.

Lin, C. J., P. Pongprueksa, S. E. Lindberg, S. O. Pehkonen, D. Byun, and C. Jang (2006), Scientific uncertainties in atmospheric mercury models I: Model science and evaluation, *Atmos. Environ.*, *40*, 2911–2928.

Lindqvist, O., K. Johansson, M. Aastrup, A. Andersson, L. Bringmark, G. Hovsenius, L. Hakanson, A. Iverfeldt, M. Meili, and B. Timm (1991), Mercury in the Swedish environment – Recent research on causes, consequences and corrective methods, *Water Air Soil Poll.*, *55*.

Lorey, P., and C. T. Driscoll (1999), Historical trends of mercury deposition in Adirondack Lakes, *Environ. Sci. Technol.*, *33*, 718–722.

Malmstrom, C. M., M. V. Thompson, G. P. Juday, S. O. Los, J. T. Randerson, and C. B. Field (1997), Interannual variation in global-scale net primary production: Testing model estimates, *Global Biogeochem. Cycles*, *11*, 367–392, doi:10.1029/97GB01419.

Mason, R. P., and G.-R. Sheu (2002), Role of the ocean in the global mercury cycle, *Global Biogeochem. Cycles*, *16*(4), 1093, doi:10.1029/2001GB001440.

Mason, R. P., W. F. Fitzgerald, and F. M. M. Morel (1994), The biogeochemical cycling of elemental mercury: Anthropogenic influences, *Geochim. Cosmochim. Acta.*, *58*, 3191–3198.

Mergler, D., H. A. Anderson, L. H. M. Chan, K. R. Mahaffey, M. Murray, M. Sakamoto, and A. H. Stern (2007), Methylmercury exposure and health effects in humans: A worldwide concern, *Ambio*, *35*, 3–11.

Millhollen, A. G., M. S. Gustin, and D. Obrist (2006), Foliar mercury accumulation and exchange for three tree species, *Environ. Sci. Technol.*, *40*, 6001–6006.

Monteiro, L. R., and R. W. Furness (2005), Seabirds as monitors of mercury in the marine environment, *Water Air Soil Poll.*, *80*, 851–870.

Moreau, J. W., and D. P. Krabbenhoft (2008), Molecular Scale Dissolved Organic Matter Interactions Impact Mercury Bioavailable for Uptake and Methylation by Sulfate-Reducing Bacteria, AGU, Fall Meeting 2008.

Obrist, D. (2007), Atmospheric mercury pollution due to losses of terrestrial carbon pools?, *Biogeochemistry*, *85*, 119–123, doi:10.1007/s10533-007-9108-0.

Obrist, D., D. W. Johnson, and S. E. Lindberg (2009), Mercury concentrations and pools in four Sierra Nevada forest sites and relationships to organic carbon and nitrogen, *Biogeosciences*, *6*, 765–777.

Pacyna, E. G., J. M. Pacyna, F. Steenhuisen, and S. Wilson (2006), Global anthropogenic mercury emission inventory for 2000, *Atmos. Environ.*, *40*, 4048–4063.

Parton, W. J., D. S. Schimel, C. V. Cole, and D. S. Ojima (1987), Analysis of factors controlling soil organic levels of grasslands in the Great Plains, *Soil Sci. Soc. Am. J.*, *51*, 1173–1179.

Pirrone, N., I. Allegrini, G. J. Keeler, J. O. Nriagu, R. Rossmann, and J. A. Robbins (1998), Historical atmospheric mercury emissions and depositions in North America compared to mercury accumulation in sedimentary records, *Atmos. Environ.*, *32*, 929–940.

Potter, C. S., J. T. Randerson, C. B. Field, P. A. Matson, P. M. Vitousek, H. A. Mooney, and S. A. Klooster (1993), Terrestrial ecosystem production: A process model based on global satellite and surface data, *Global Biogeochem. Cycles*, *7*(4), 811–841, doi:10.1029/93GB02725.

Qian, J., U. Skyllberg, W. Frech, W. F. Bleam, P. R. Bloom, and P. E. Petit (2002), Bonding of methyl mercury to reduced sulfur groups in soil and stream organic matter as determined by X-ray absorption spectroscopy and binding affinity studies, *Geochim. Cosmochim. Acta.*, *66*(22), 3873–3885.

Randerson, J. T., M. V. Thompson, C. M. Malmstrom, C. B. Field, and I. Y. Fung (1996), Substrate limitations for heterotrophs: Implications for models that estimate the seasonal cycle of atmospheric CO2, *Global Biogeochem. Cycles*, *10*(4), 585–602, doi:10.1029/96GB01981.

Rea, A. W., S. E. Lindberg, T. Scherbatoxkoy, and G. J. Keeler (2002), Mercury accumulation in foliage over time in two northern mixed-hardwood forests, *Water Air Soil Poll.*, *133*(1–4), 49–67.

Rolfhus, K. R., and W. F. Fitzgerald (2004), Mechanisms and temporal variability of dissolved gaseous mercury production in coastal seawater, *Mar. Chem.*, *90*, 125–136.

Ruimy, A., L. Kergoat, and A. Bondeau (1999), Comparing global models of terrestrial net primary productivity (NPP): analysis of difference in light absorption and light use efficiency, *Global Change Biol.*, *5*, 56–64.

Schroeder, W. H., S. Beauchamp, G. Edwards, L. Poissant, P. Rasmussen, R. Tordon, G. Dias, J. Kemp, B. van Heyst, and C. M. Banic (2005), Gaseous mercury emissions from natural sources in Canadian landscapes, *J. Geophys. Res.*, *110*, D18302, doi:10.1029/2004JD005699.

Seigneur, C., K. Vijayaraghavan, K. Lohman, P. Karamchandani, and C. Scott (2004), Global source attribution for mercury deposition in the United States, *Environ. Sci. Technol.*, *38*, 555–569.

Selin, N. E., and D. J. Jacob (2008), Seasonal and spatial patterns of mercury wet deposition in the United States: Constraints on the contribution from North American anthropogenic sources, *Atmos. Environ.*, *42*, 5193–5204.

Selin, N. E., D. J. Jacob, R. J. Park, R. M. Yantosca, S. Strode, L. Jaegle, and D. Jaffe (2007), Chemical cycling and deposition of atmospheric mercury: Global constraints from observations, *J. Geophys. Res.*, *112*, D02308, doi:10.1029/2006JD007450.

Selin, N. E., D. J. Jacob, R. M. Yantosca, S. Strode, L. Jaegle, and E. M. Sunderland (2008), Global 3-D land-ocean-atmosphere model for mercury: Present-day versus preindustrial cycles and anthropogenic enrichment factors for deposition, *Global Biogeochem. Cycles*, *22*, GB2011, doi:10.1029/2007GB003040.

Shia, R.-L., C. Seigneur, P. Pai, M. Ko, and N. D. Sze (1999), Global simulation of atmospheric mercury concentrations and deposition fluxes, *J. Geophys. Res.*, *104*, 23,747–23,760, doi:10.1029/1999JD900354.

Skyllberg, U., K. Xia, P. R. Bloom, N. A. Nater, and W. F. Bleam (2000), Binding of mercury(II) to reduced sulfur in soil organic matter along upland-peat soil transects, *J. Environ. Qual.*, *29*, 855–865.

Skyllberg, U., J. Qian, W. Frech, K. Xia, and W. Bleam (2003), Distribution of mercury, methyl mercury and organic sulphur species in soil, soil solution and stream of a boreal forest catchment, *Biogeochemistry*, *64*(1), 53–76.

Smith, D. B., W. F. Cannon, L. G. Woodruff, R. G. Garrett, R. Klassen, J. E. Kilburn, J. D. Horton, H. D. King, M. B. Goldhaber, and J. M. Morrison (2005), Major- and Trace-Element concentrations in soils from two continental scale transects of the United States and Canada, *USGS Open-File Report 2005-1253*.

Stamenkovic, J., and M. S. Gustin (2009), Nonstomal versus stomatal uptake of atmospheric mercury, *Environ. Sci. Technol.*, *43*, 1367–1372, doi:10.1021/es801583a.

Strode, S. A., L. Jaegle, N. E. Selin, D. J. Jacob, R. J. Park, R. M. Yantosca, R. P. Mason, and F. Slemr (2007), Air-sea exchange in the global mercury cycle, *Global Biogeochem. Cycles*, *21*, GB1017, doi:10.1029/2006GB002766.

Sunderland, E. M., and R. P. Mason (2007), Human impacts on open ocean mercury concentrations, *Global Biogeochem. Cycles*, *21*, GB4022, doi:10.1029/2006GB002876.

Swain, E. B., D. R. Engstrom, M. E. Brigham, T. A. Henning, and P. L. Brezonik (1992), Increasing rates of atmospheric mercury deposition in mid continental North America, *Science*, *257*, 784–787.

Turetsky, M. R., J. W. Harden, H. R. Friedli, M. Flannigan, N. Payne, J. Crock, and L. Radke (2006), Wildfires threaten mercury stocks in northern soils, *Geophys. Res. Lett.*, *33*, L16403, doi:10.1029/2005GL025595.

van der Werf, G. R., J. T. Randerson, G. J. Collatz, and L. Giglio (2003), Carbon emissions from fires in tropical and subtropical ecosystems, *Global Change Biol.*, *9*(4), 547–562.

van der Werf, G. R., J. T. Randerson, L. Giglio, G. J. Collatz, P. S. Kasibhatla, and A. F. Arellano (2006), Interannual variability in global biomass burning emissions from 1997 to 2004, *Atmos. Chem. Phys.*, *6*, 3423–3441.

Wang, Y., D. J. Jacob, and J. A. Logan (1998), Global simulation of tropospheric O_3-NO_x-hydrocarbon chemistry: 1. Model formulation, *J. Geopys. Res.*, *103*, 10,713–10,726.

Wesely, M. L. (1989), Parameterization of surface resistances to gaseous dry deposition in regional-scale numerical-models, *Atmos. Environ.*, *23*, 1293–1304.

Wickland, K., D. Krabbenhoft, and S. Olund (2006), Evidence for a link between soil respiration and mercury emission from organic soils, *Abstracts of the 8th international conference on mercury as a global pollutant*, Madison, August 6–11, 2006.

Wiedinmyer, C., and H. Friedli (2007), Mercury emission estimates from fires: An initial inventory for the United States, *Environ. Sci. Technol.*, *41*, 8092–8098, doi:10.1021/es071289o.

D. J. Jacob and E. M. Sunderland, Faculty of Arts and Sciences, Harvard University, Cambridge, MA 02138, USA.

N. V Smith-Downey, Jackson School of Geosciences, University of Texas, Austin, TX 78758, USA. (nicolevdowney@gmail.com)